Psychoradiology, 2023, **3**, 1–12
DOI: 10.1093/psyrad/kkad016
Advance access publication date: 13 October 2023
Research Article

The right inferior frontal gyrus as pivotal node and effective regulator of the basal ganglia-thalamocortical response inhibition circuit

Qian Zhuang[1,2,#], Lei Qiao[3,#], Lei Xu[1,4], Shuxia Yao[1], Shuaiyu Chen[2], Xiaoxiao Zheng[1,5], Jialin Li[1], Meina Fu[1], Keshuang Li[1,6], Deniz Vatansever[7], Stefania Ferraro[1], Keith M. Kendrick[1,7,*] and Benjamin Becker[8,9,*]

[1]The Center of Psychosomatic Medicine, Sichuan Provincial Center for Mental Health, Sichuan Provincial People's Hospital, The University of Electronic Science and Technology of China, Chengdu, Sichuan Province 611731, China
[2]Center for Cognition and Brain Disorders, The Affiliated Hospital of Hangzhou Normal University, Hangzhou, Zhejiang Province 311121, China
[3]School of Psychology, Shenzhen University, Shenzhen 518060, China
[4]Institute of Brain and Psychological Sciences, Sichuan Normal University, Chengdu, 610068, China
[5]Brain Cognition and Brain Disease Institute (BCBDI), Shenzhen Institute of Advanced Technology, Chinese Academy of Sciences, Shenzhen 518055, China
[6]School of Psychology and Cognitive Science, East China Normal University, Shanghai 200062, China
[7]Institute of Science and Technology for Brain-Inspired Intelligence, Fudan University, Shanghai 200433, China
[8]State Key Laboratory of Brain and Cognitive Sciences, The University of Hong Kong, Hong Kong 999077, China
[9]Department of Psychology, The University of Hong Kong, Hong Kong 999077, China
*Correspondence: Benjamin Becker, bbecker@hku.hk; Keith M. Kendrick, k.kendrick.uestc@gmail.com
[#]Qian Zhuang and Lei Qiao are joint first author.

Abstract

Background: The involvement of specific basal ganglia-thalamocortical circuits in response inhibition has been extensively mapped in animal models. However, the pivotal nodes and directed causal regulation within this inhibitory circuit in humans remains controversial.

Objective: The main aim of the present study was to determine the causal information flow and critical nodes in the basal ganglia-thalamocortical inhibitory circuits and also to examine whether these are modulated by biological factors (i.e. sex) and behavioral performance.

Methods: Here, we capitalize on the recent progress in robust and biologically plausible directed causal modeling (DCM-PEB) and a large response inhibition dataset ($n = 250$) acquired with concomitant functional magnetic resonance imaging to determine key nodes, their causal regulation and modulation via biological variables (sex) and inhibitory performance in the inhibitory circuit encompassing the right inferior frontal gyrus (rIFG), caudate nucleus (rCau), globus pallidum (rGP), and thalamus (rThal).

Results: The entire neural circuit exhibited high intrinsic connectivity and response inhibition critically increased causal projections from the rIFG to both rCau and rThal. Direct comparison further demonstrated that response inhibition induced an increasing rIFG inflow and increased the causal regulation of this region over the rCau and rThal. In addition, sex and performance influenced the functional architecture of the regulatory circuits such that women displayed increased rThal self-inhibition and decreased rThal to GP modulation, while better inhibitory performance was associated with stronger rThal to rIFG communication. Furthermore, control analyses did not reveal a similar key communication in a left lateralized model.

Conclusions: Together, these findings indicate a pivotal role of the rIFG as input and causal regulator of subcortical response inhibition nodes.

Keywords: response inhibition; basal ganglia; inferior frontal gyrus; effective connectivity; DCM

Introduction

Animal models and human neuroimaging studies convergently demonstrated that inhibitory control critically relies on highly specific basal ganglia-thalamocortical circuits (Alexander *et al.*, 1986, 1991; Alexander and Crutcher, 1990; Aron *et al.*, 2007; Jahfari *et al.*, 2019; Morein-Zamir and Robbins, 2015; Pfeifer *et al.*, 2022; Schall and Godlove, 2012; Stuphorn, 2015; Verbruggen and Logan, 2009; Wei and Wang, 2016). Dysregulations in this circuit have been implicated in disorders characterized by inhibitory control deficits, including addiction (Klugah-Brown *et al.*, 2020; Morein-Zamir and Robbins, 2015; Zhou *et al.*, 2018), attention deficit/hyperactivity (ADHD, Morein-Zamir *et al.*, 2014; Sonuga-Barke, 2005), schizophrenia (Camchong *et al.*, 2006; Feng *et al.*, 2018; Mamah *et al.*, 2007), and Parkinson disorder (DeLong and Wichmann, 2015; Obeso *et al.*, 2000).

The key nodes within this response inhibition circuitry have been extensively mapped with convergent evidence suggesting critical contributions from the pre-supplementary motor area (pre-SMA) and lateral prefrontal cortex (lPFC), in particular, the inferior frontal gyrus (IFG) (Aron *et al.*, 2003; Dambacher *et al.*, 2014; Hampshire *et al.*, 2010; Maizey *et al.*, 2020; Schaum *et al.*, 2021; Verbruggen and Logan, 2008; Zhang *et al.*, 2017) and the striatal regions including the caudate and putamen (Eagle *et al.*, 2011; Ghahremani *et al.*, 2012; Hampton *et al.*, 2017; Kelly *et al.*, 2004;

Received: 26 May 2023; **Revised:** 13 August 2023; **Accepted:** 12 September 2023

Ott and Nieder, 2019; Robertson *et al.*, 2015; Robbins, 2007). Importantly, consistent evidence has demonstrated that enhanced behavioral response inhibition was closely associated with increased connectivity strength in the IFG–striatal pathway (Jahfari *et al.*, 2011; Xu *et al.*, 2016). Furthermore, anatomical and neurochemical studies suggest that response inhibitory control within the fronto-striatal circuitry is modulated by dopaminergic and noradrenergic signaling (Bari *et al.*, 2011; Ghahremani *et al.*, 2012; Li *et al.*, 2020; Pfeifer *et al.*, 2022; Rae *et al.*, 2016; Robertson *et al.*, 2015). Such as, dopamine receptor availability in the fronto-striatal circuits is significantly related to inhibition-related neural responses (Ghahremani *et al.*, 2012; Pfeifer *et al.*, 2022). While the dorsal striatum represents an important locus of dopaminergic control of response inhibition (Ghahremani *et al.*, 2012; Robertson *et al.*, 2015), dopamine receptor availability in the lPFC modulates motor control via downstream regulatory projections to the striatum (Ott and Nieder, 2019; Vijayraghavan *et al.*, 2016). On the other hand, enhanced norepinephrine signaling facilitates response inhibition via modulation of the IFG and its connections with the striatum (Chamberlain *et al.*, 2009; Rae *et al.*, 2016), during which the IFG plays an important role in top-down control of the basal ganglia regions (Buschman and Miller, 2014; Hampshire *et al.*, 2010; Jahfari *et al.*, 2012; Kim, 2014; Puiu *et al.*, 2020; Renteria *et al.*, 2018; Schaum *et al.*, 2021; Tops and Boksem, 2011).

A large number of studies have demonstrated the pivotal role of the thalamus in the basal ganglia-thalamocortical model of response inhibition (Alexander *et al.*, 1986, 1991; Alexander and Crutcher, 1990). Specifically, the thalamus relays information between the basal ganglia and cortex (Collins *et al.*, 2018; Haber and Mcfarland, 2001; Haber and Calzavara, 2009; McFarland and Haber, 2002)—thus facilitating response inhibition and performance monitoring (Bosch-Bouju *et al.*, 2013; Huang *et al.*, 2018; Saalmann and Kastner, 2015; Tanaka and Kunimatsu, 2011)—via dense reciprocal connections with the basal ganglia and PFC (Guillery, 1995; Phillips *et al.*, 2021; Xiao *et al.*, 2009; Tanaka and Kunimatsu, 2011).

Consistent findings from animal model and human neuroimaging studies show that the globus pallidus (GP) also plays an essential role in action execution and response inhibition (Casey *et al.*, 1997; Mallet *et al.*, 2016; Pan *et al.*, 2018; Wei and Wang, 2016). A previous structural imaging study revealed that a better behavioral performance during a response inhibition task was related to a larger GP volume (Casey *et al.*, 1997). In addition, a study from Wei and Wang showed that GABAergic inhibitory projections from the external segment of the GP to the striatum are crucial for inhibiting a planned response (Wei and Wang, 2016).

Several studies have explored sex differences in response inhibition performance and the associated neural activity (Chung *et al.*, 2020; Ribeiro *et al.*, 2021; Rubia *et al.*, 2013; Sjoberg and Cole, 2018). While the existing evidence from most studies and meta-analyses showed no significant sex difference on behavioral performance (Chung *et al.*, 2020; Cross *et al.*, 2011; Gaillard *et al.*, 2021; Garavan *et al.*, 2006; Li *et al.*, 2006), some other studies showed that female individuals demonstrate higher accuracy and faster stop signal reaction times compared to male participants (Ribeiro *et al.*, 2021; Rubia *et al.*, 2013; Sjoberg and Cole, 2018) and one study reported that males demonstrate better response inhibition compared to females (Gaillard *et al.*, 2020). With respect to neural differences the previous literature remained inconsistent and the direction of sex differences may additionally vary depending on the task administered (Go/NoGo task or stop signal task) and the age of the participants (Chung *et al.*, 2020; Rubia *et al.*, 2013; Weafer, 2020). Such as, some studies reported that male participants tend to display greater brain activity in frontal as well as motor control-related regions such as the GP and thalamus during response inhibition on stop signal tasks when inhibiting an already-initiated response (Li *et al.*, 2006, 2009), while female participants tend to display greater brain activity during inhibition on Go/NoGo tasks when inhibiting the initiation of a response (Chung *et al.*, 2020; Garavan *et al.*, 2006).

Convergent evidence from human lesion studies and neuroimaging meta-analyses demonstrates a right-lateralized inhibitory control network encompassing the right IFG (rIFG), right caudate nucleus (rCau), right GP (rGP), and right thalamus (rThal) (Aron *et al.*, 2003; Chevrier *et al.*, 2007; Garavan *et al.*, 1999; Hung *et al.*, 2018; Jahfari *et al.*, 2011; Thompson *et al.*, 2021). However, while extensive research has highlighted the critical role of these regions within a right-lateralized inhibitory control circuitry, the causal information flow and critical contribution of single nodes within this network as well as the modulatory effect of sex have not been determined.

We therefore capitalized on a novel dynamic causal modeling (DCM) approach based on *a priori* specification of biologically and anatomically plausible models that allows estimation of directed causal influences between nodes and their modulation by changing task demands (Friston *et al.*, 2003; Stephan *et al.*, 2010) in the largest sample to date ($n = 250$). The DCM approach conceptualizes the brain as a nonlinear dynamical input-state-output system and was developed to provide a more biologically informed approach to test a hypothesis about experimental manipulation-dependent interactions between brain regions based on differential equations describing interactions between neural populations that may directly or indirectly give rise to the observed functional magnetic resonance imaging (fMRI) data. The estimated parameters in these models are considered as directed or effective connectivity between brain regions. DCM further allows comparison of modulatory effective connectivity strength across different experimental conditions using Bayesian contrasts (Dijkstra *et al.*, 2017) and, in combination with the recently developed parametrical empirical Bayes (PEB) hierarchical framework (DCM-PEB method), it allows modeling of both commonalities and differences in effective connectivity between participants, e.g. to determine the neurobiological basis of sex and behavioral performance variations (Friston *et al.*, 2016; Zeidman *et al.*, 2019a, 2019b).

To determine the causal information flow and critical nodes in the basal ganglia-thalamocortical circuits and whether these are modulated by biological factors (i.e. sex) and show functional relevance in terms of associations with performance we capitalized on DCM-PEB in combination with fMRI data collected in a large sample of healthy individuals ($n = 250$) during a well-established response inhibition paradigm (emotional Go/NoGo task, see also Zhuang *et al.*, 2021). To unravel the key nodes and causal influences within the inhibitory control network, we first estimated the effective connectivity between and within key regions involved in response inhibitory control within the rIFG-rCau-rGP-rThal functional circuit (right lateralized model) and, second, we estimated sex differences and behavioral performance effects on connectivity parameters. Furthermore, to validate the hemispheric asymmetry of the inhibitory control network, an identical model of nodes was tested in the left hemisphere (left lateralized model).

Given convergent evidence on a pivotal role of the right IFG in mediating top-down cortical–subcortical control via connectivity pathways with striatal and thalamic areas during response inhibition (Aron *et al.*, 2003; Dambacher *et al.*, 2014; Hampshire *et al.*, 2010; Maizey *et al.*, 2020), we predicted a greater modulatory effect on rIFG and its directed connectivity to both rCau

and rThal in the NoGo compared to Go condition. Additionally, based on previous studies reporting sex differences in both, behavioral response inhibition and associated neural processing in cortical-subcortical circuits (i.e. sex, Li *et al.*, 2006; Ribeiro *et al.*, 2021; Sjoberg and Cole, 2018), as well as a significant correlation between enhanced inhibitory control and increased frontal-striatal connectivity (Chang *et al.*, 2020; Jahfari *et al.*, 2011; Wei and Wang, 2016; Xu *et al.*, 2016), we hypothesized a modulation of the key pathways by biological and performance variations with better response inhibition being associated with stronger causal regulation in the inhibition circuitry, especially in the IFG-Cau pathway. Finally, in line with consistent evidence that showed right-lateralized brain areas and neural circuits involved in the response inhibition (Aron *et al.*, 2003; Chevrier *et al.*, 2007; Hung *et al.*, 2018; Jahfari *et al.*, 2011; Thompson *et al.*, 2021), we proposed a different causal structure for the left and right models given the hemispheric asymmetry in the inhibitory network.

Materials and Methods

Participants

In this study, $n = 250$ healthy right-handed participants were enrolled and underwent a validated Go/NoGo fMRI paradigm. The data have been previously used to examine undirected functional connectivity within domain-general and emotion-specific inhibitory brain systems (Zhuang *et al.*, 2021), and were part of a larger neuroimaging project examining pain empathy (Li *et al.*, 2019 ; Zhou *et al.*, 2020), emotional face memory (Liu *et al.*, 2022), and mirror neuron processing (Xu *et al.*, 2022). After quality assessment during the processes of data collection and preprocessing $n = 218$ participants were included (104 males, details see Supplementary Materials). During the model estimation processes, explained variance by the specified model on the individual level was calculated with higher values reflecting better model inversion (Zeidman *et al.*, 2019a). In line with previous studies (Bencivenga *et al.*, 2021; Rupprechter *et al.*, 2020), participants with <10% of explained variance were excluded and finally a total of 118 participants (56 males, age: mean ± SEM = 21.57 ± 0.21 years) were included into further analyses. The study was approved by the local ethics committee and in accordance with the latest version of the Declaration of Helsinki.

Response Inhibition Paradigm

A validated mixed event-related block design linguistic emotional Go/NoGo fMRI paradigm was employed (Goldstein *et al.*, 2007; Prototopopescu *et al.*, 2005, for details see Zhuang *et al.*, 2021). Notably, although both the Go/NoGo and stop signal paradigm are commonly used to examine response inhibition control and associated brain function, the former paradigm captures action restraint while the latter primarily involves action cancellation (Raud *et al.*, 2020; Schachar *et al.*, 2007). During the present Go/NoGo task, participants were required to make responses as accurately and quickly as possible based on orthographical cues, i.e. words were presented in normal or italic font. For words in a normal font, participants were instructed to perform a button-press (Go trials), while inhibiting their response to words presented in italic font (NoGo trials). Omission errors were defined when no responses were made for Go trials, while commission errors were defined when responses were made to NoGo trials. Positive, negative, and neutral words were included into the paradigm as stimuli. However, given that the main aim of the present study was to examine the causal influence within the general inhibition network as proposed by Alexander *et al.* (1986, 1991; Alexander and Crutcher, 1990) and to increase statistical power in this respect the different emotional valence conditions (e.g. positive Go condition, positive NoGo condition, negative Go condition, negative NoGo condition, neutral Go condition, and neutral NoGo condition) were not further accounted for in the DCM analysis. Stimuli were presented in two runs and each run included 12 blocks (six blocks: Go; six blocks: NoGo). Each Go block encompassed 18 normal font words (100% Go trials) while each NoGo block encompassed 12 normal font words (66.7% Go trials) and six italicized font words (33.3% NoGo trials). Further details can be found in Zhuang *et al.* (2021) and the Supplementary Materials.

Behavioral Data Analysis

In our previous study, we demonstrated that participants exhibited more commission errors during inhibitory control (i.e. NoGo > Go) as well as faster responses in positive Go contexts and lower accuracy in positive NoGo contexts (Zhuang *et al.*, 2021). Given that sex-differences were examined in the DCM model, the present analyses additionally examined sex-differences on accuracy and reaction times (Supplementary Materials). Given previous studies have showed age-related effects on inhibition (Rey-Mermet *et al.*, 2018; Rubia *et al.*, 2007) age was included as covariate.

MRI Data Acquisition and Preprocessing

MRI data were collected on a 3T MRI system using standard sequences and were initially preprocessed using validated protocols in SPM 12 (for details see Supplementary Materials).

GLM Analysis

An event-related general linear model (GLM) was established in SPM12. To examine domain general inhibitory control (irrespective of emotional context) the overarching inhibitory control contrast was modeled (e.g. all NoGo > all Go trials) and convolved with the canonical hemodynamic response function. Six head motion parameters were included in the design matrix to control movement-related artifacts and a high-pass filter (1/128 Hz) was applied to remove low frequency components. The contrast of interest (contrast: NoGo > Go) was created and subjected to one-sample *t*-test at the second level. In line with previous studies (Aron *et al.*, 2003; Chevrier *et al.*, 2007; Hung *et al.*, 2018; Jahfari *et al.*, 2011; Thompson *et al.*, 2021), group-level (contrast: NoGo > Go) peaks in the IFG, Cau, GP, and Thal within the identified general inhibition network were then used to define individual-specific regions of interest (ROI) for the DCM analysis. Additionally, a two-sample *t*-test was conducted (contrast: NoGo > Go) to examine sex-dependent effects on the response inhibition network. Analyses were corrected for multiple comparisons using a conservative peak-level threshold on the whole brain level ($P < 0.05$ family-wise error, FWE).

DCM and Node Definition

A DCM analysis was employed to determine directed causal influences according to the circuitry model proposed by Alexander *et al.* (1986, 1991; Alexander and Crutcher, 1990). The DCM approach allows construction of a realistic neuronal model of interacting regions and the prediction of the underlying neuronal activity from the measured hemodynamic response (Friston *et al.*, 2003; Stephan *et al.*, 2007). To this end, directed causal influences between the key regions including IFG, Cau, GP, and Thal in the basal ganglia-thalamocortical loop and their modulation via experimental manipulations (engagement of motor inhibitory control) were examined. In line with previous neuroimaging studies

and meta-analyses demonstrating a right-lateralized inhibition model (right model) encompassing the rIFG, rCau, rGP, and rThal (Aron *et al.*, 2003; Chevrier *et al.*, 2007; Hung *et al.*, 2018; Jahfari *et al.*, 2011; Thompson *et al.*, 2021), our main hypothesis testing focused on the right lateralized network. To further validate the hemispheric asymmetry of the inhibitory control network an identical model was tested for the left hemisphere including the lIFG, lCau, lGP, and lThal. In line with previous studies, we combined atlas-based masks (Human Brainnetome Atlas, Fan *et al.*, 2016) with group-level and individual level activity maps to generate the corresponding nodes (Fernández-Espejo *et al.*, 2015; Holmes *et al.*, 2021; Qiao *et al.*, 2020; Van Overwalle *et al.*, 2020). Among this, the caudate is limited to a mask that combines the ventral and dorsal caudate but not the putamen (Fan *et al.*, 2016).

Model Specification and Estimation

A two-step DCM analysis was performed using the DCM-parametric empirical Bayes (PEB) approach (Zeidman *et al.*, 2019a, 2019b). On the first-level, time-series from four ROI (rIFG, rCau, rGP, rThal) were extracted. A full DCM model was specified for each participant and all connectivity parameters in both forward (e.g. rIFG-rThal-rGP-rCau-rIFG) and backward (e.g. rIFG-rCau-rGP-rThal-rIFG) directions were estimated. We estimated three key DCM parameters: (i) the matrix A reflecting all connections including forward and backward connectivity between ROI and self-inhibitions in each ROI, (ii) the matrix B representing modulatory effects of Go and NoGo condition on all connections, and (iii) the matrix C representing the driving inputs into ROI from Go and NoGo conditions separately. Given that all inputs in the model were mean-centered, intrinsic connectivity in the matrix A indicates mean effective connectivity independent of all experimental conditions. The model was estimated using variational Laplace (Friston *et al.*, 2007). Further details are presented in the Supplementary Material. At the second (group) level, we constructed a PEB model over the first-level estimated parameters. In accordance with previous studies (Bencivenga *et al.*, 2021; Rupprechter *et al.*, 2020), we evaluated the explained variance by the model on the individual level (Zeidman *et al.*, 2019a)—and then we only included participants with >10% of explained variance in the PEB model. Finally, 118 participants were included for further analyses.The number of excluded participants is similar to a previous study (Rupprechter *et al.*, 2020). The differences on behavioral performance were examined between the excluded and included participants and no significant differences were found (all $P \geq 0.23$, for details see the Supplementary Material), suggesting no evidence of biased selection.

The primary aim of the present study was to establish a causal neurobiological model for response inhibition and to determine the interaction between key players in this circuitry. To evaluate the model three PEB analyses were carried out separately for A, B, and C matrices. Separate analyses examined sex and performance variations (for details, see the Supplementary Materials).

Next, to identify the model that best represented our data, Bayesian model reduction was performed to compare the free energy of the full model with numerous reduced models for which specific parameters were "switched off" (Friston *et al.*, 2016). An automatic greedy search procedure (iterative procedure) was employed to facilitate an efficient comparison of thousands of models. In this procedure, parameters that do not contribute to free energy were pruned away. Next, the Bayesian model average, performing a weighted average of the parameters of each model, was calculated over the 256 models obtained from the final iteration (Friston *et al.*, 2016).

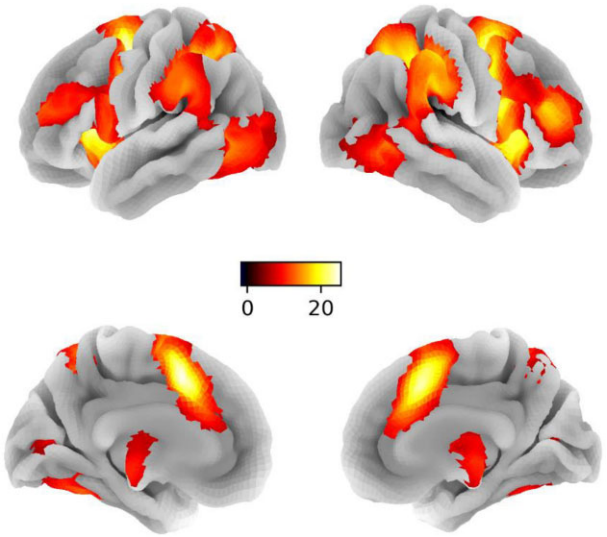

Figure 1: Brain activation maps for general response inhibition on whole brain level (contrast: NoGo > Go; $P < 0.05$ FWE, peak level). L, left; R, right. The color bar represents the *t*-values of the BOLD signal and reflect the significance level of the contrast.

Finally, to compare the effective connection strength, especially the cortical-subcortical connectivity and driving inputs into each region from different experimental conditions (NoGo and Go conditions), Bayesian contrasts (Dijkstra *et al.*, 2017) were computed over parameters from the B and C matrices. Group-level estimated parameters were thresholded at posterior probability >95% (indicating strong evidence: Kass and Raftery, 1995) based on free energy.

Results

Behavioral Results

The two-way repeated-measures ANOVA on accuracy found a significant main effect of inhibition [$F(1115) = 21.73$, $P < 0.001$, $\eta_p^2 = 0.16$], with a higher accuracy for Go compared to NoGo trials (Go trials: mean ± SEM = 98.47% ± 0.31, No Go trials: mean ± SEM = 70.34% ±1.44, Cohen's $d = 2.48$). No sex differences were found for accuracy or reaction times ($P > 0.18$). The mean reaction time for correct Go trials is mean ± SEM = 314.44, ms ± 4.94.

BOLD Activation (GLM) Analysis

Examination of domain general inhibition (contrast: NoGo > Go) revealed a widespread fronto-parietal cortical and thalamo-striatal subcortical network including the IFG, striatal, pallidal, and thalamic regions (Fig. 1 and Table 1) during response inhibition. Group-level peaks in the rIFG, rCau, rGP, and rThal were selected as centers of the ROI for model testing (Fig. 2a and Table 2). No significant sex difference was observed in blood oxygen level-dependent (BOLD) activation.

Causal Connectivity (DCM) Analysis

For the matrix A, the diagonal cells represent self-connections that are unitless log scaling parameters and were multiplied with the default value of −0.5 Hz (Zeidman *et al.*, 2019a). Positive values indicate increased self-inhibition due to task condition and

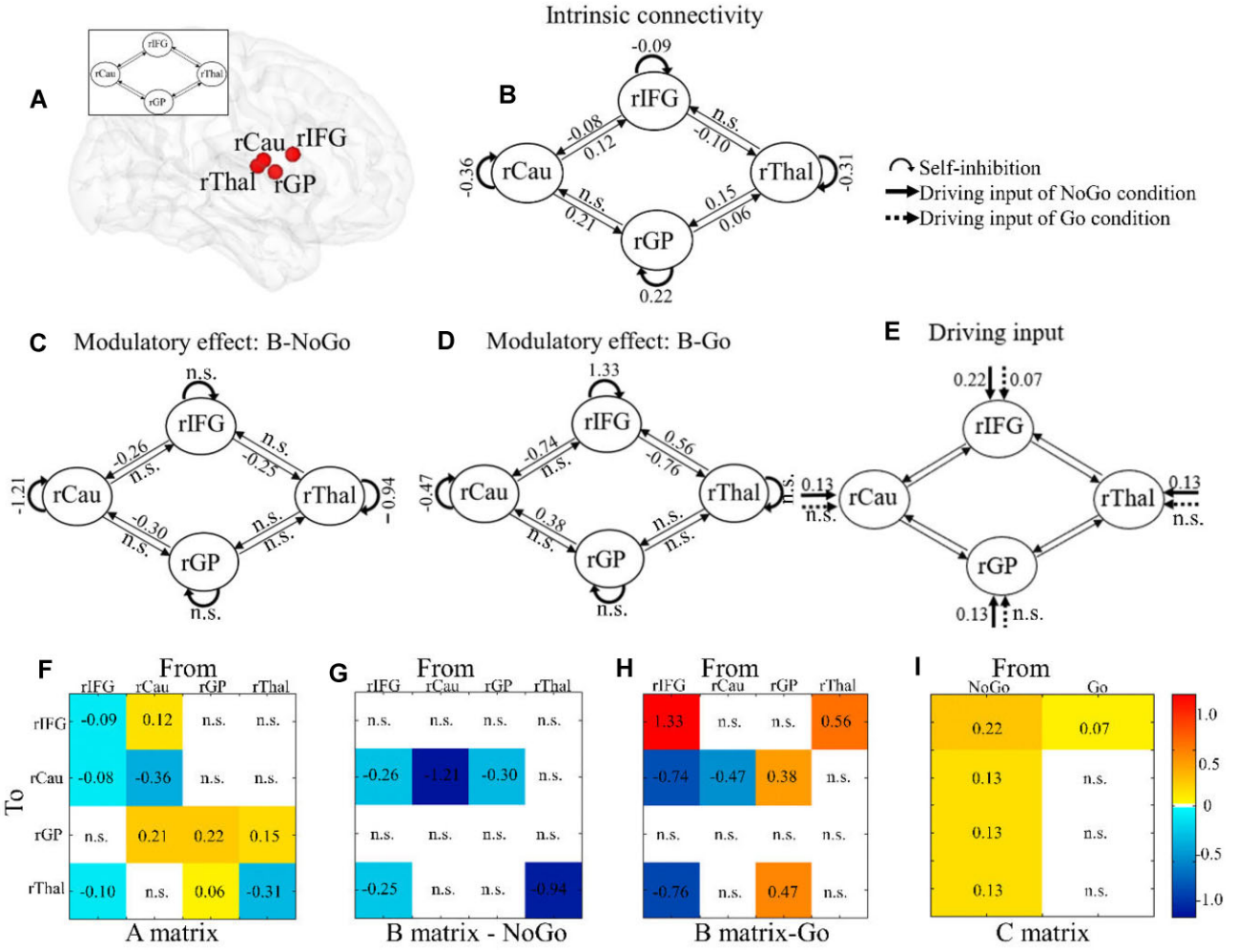

Figure 2: Location of regions included in the right model and group-level connectivity parameters. (**A**) Location of regions included in the right model. The A matrix: intrinsic connectivity across all experimental conditions (**B**, **F**). The B matrix: modulatory effect on effective connectivity between regions and self-inhibitions from NoGo (**C**, **G**) and Go condition (**D**, **H**). The C matrix: Driving inputs in ROI in the NoGo and Go condition (**E**, *I*). Values in matrices reflect the connectivity parameters. Effective connectivity strengths are displayed by the color ranging from yellow to dark red (i.e. excitatory connectivity) and from turquoise to dark blue (i.e. inhibitory). Parameters with stronger evidence (posterior probability >95%) are presented and subthreshold parameters are marked with "n.s.".

Table 1: Regions involved in the domain general inhibition control on the group level (contrast: NoGo > Go).

Regions	Cluster *k*	Coordinates			*t* value
		x	y	z	
Frontal lobe including MFG and SFG extending to parietal, temporal and occipital lobe	19 718	27	3	51	25.40
		18	6	57	25.05
		−3	12	45	24.55
mOFC	72	27	45	−21	8.67
lCalcarine	152	−12	−75	9	8.44
rCalcarine	61	15	−72	9	6.57

Note: Group level brain activation maps involved in the domain general inhibition control (contrast: NoGo > Go, peak level, $p_{FWE} < 0.05$). MFG, middle frontal gyrus; SFG, superior frontal Gyrus; mOFC, middle orbital frontal cortex; r, right; l, left.

Table 2: Activation and peak values for key regions included in the right model.

Regions	Cluster *K*	Coordinates			*t*-value
		x	y	z	
rIFG	611	51	12	18	21.40
rCau	144	15	−3	15	13.61
rGP	63	21	−3	9	12.43
rThal	340	15	−6	12	14.30

Note: Key nodes including rIFG, rCau, rGP, and rThal survived from the overlay between image masks of corresponding regions defined by Human Brainnetome Atlas and group level brain activation maps (peak level, $p_{FWE} < 0.05$) and thus served as ROI combined with the individual peak location search on the individual level. Cau, caudate nucleus; GP, global pallidum; r, right; Thal, thalamus.

decreased responsivity to the inputs from the other regions of the network, while negative values indicate decreased self-inhibition and increased responsivity to the inputs from other nodes of the network (Zeidman *et al.*, 2019a). Our findings revealed negative self-inhibition values for the rIFG, rCau, and rThal but a positive value for the rGP (Fig. 2b,f), indicating that the GP increased self-connection while the other nodes increased interaction with other nodes in the network.

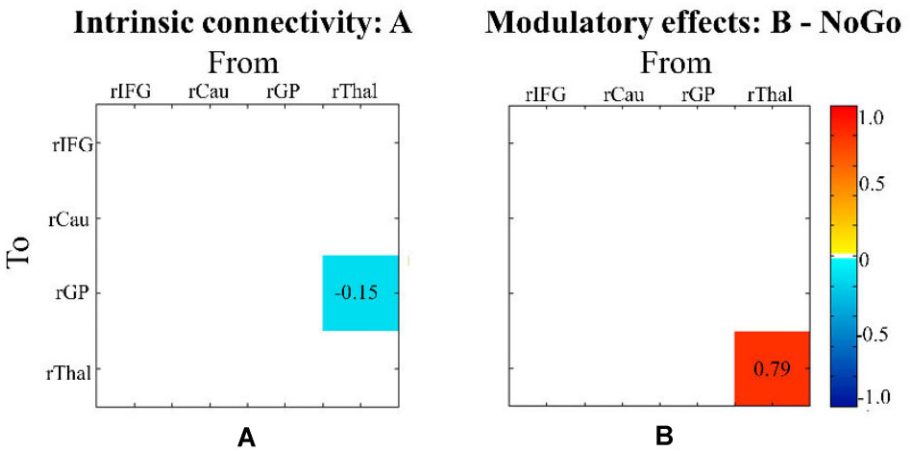

Figure 3: Sex effect on connectivity parameters in terms of A matrix and B matrix. (**A**) For intrinsic connectivity in A matrix, female participants showed a more negative influence from rThal to rGP compared to male participants. (**B**) In the NoGo condition, there is a greater self-inhibition in rThal in female than male participants in terms of B matrix. Effective connectivity strengths are displayed by the color ranging from yellow to dark red (i.e. excitatory connectivity) and from turquoise to dark blue (i.e. inhibitory). Parameters with stronger evidence (posterior probability > 95%) are presented.

For the off-diagonal cells in the matrix A, the values (in Hz) reflect the rate of change in the activity of the target region caused by the source region per second. Positive values reflect excitatory effects while negative values indicate inhibitory effects. In the forward direction (e.g. rIFG-rThal-rGP-rCau-rIFG), we found a significant negative connectivity from rIFG to rThal and positive connectivity from rThal to rGP as well as rCau to rIFG. In the backward direction (e.g. rIFG-rCau-rGP-rThal-rIFG), rIFG exhibited a negative inhibitory influence onto rCau, alongside an excitatory connection from rCau to rGP and rGP to rThal (Fig. 2b,f). Although the connectivity from rThal to rIFG was not significant, a weak evidence (posterior probability of 57%) for this connection was observed with a more lenient threshold.

Values in the matrix B represent the rate of change, in Hz, in the connectivity from source area to target area induced by the experimental conditions (Zeidman *et al.*, 2019a). During inhibitory control (NoGo condition) the rIFG exerted a negative influence onto the rCau and rThal whereas the rGP exerted a negative influence on the rCau (Fig. 2c,g). In addition, we found negative self-inhibition values in both rCau and rThal, respectively. During the Go condition a negative influence of the rIFG on both rCau and rThal was observed (Fig. 2d,h), while the positive influence was observed from the rGP to rCau and from rThal to rIFG. Moreover, we found a positive self-inhibition value in rIFG and a negative value in rCau. A Bayesian contrast (NoGo > Go) allowed us to compare the connectivity strength modulation during the different experimental conditions and revealed a very strong evidence (posterior probability > 99%) that the causal influence of the rIFG to both, the rCau and rThal was stronger during inhibitory control (NoGo vs Go condition). This reflects that response inhibition critically requires a causal top-down cortical-subcortical regulation via the right IFG. We additionally found a very strong evidence (posterior probability > 99%) for a considerably stronger inhibitory connectivity from rGP to rCau in the NoGo compared to Go condition.

The matrix C represents the rate of change in neural response of one brain region due to the driving input from an experimental condition (Zeidman *et al.*, 2019a). During inhibitory control (NoGo) all regions (rIFG, rCau, rGP, and rThal) exhibited excitatory driving input while during the Go condition only the rIFG exhibited excitatory input (Fig. 2e,i). Bayesian contrasts directly comparing the conditions (NoGo > Go) demonstrated an increasing driving input specifically in the rIFG during engagement of cognitive control (NoGo > Go condition) with a 100% posterior probability.

Sex Differences in Connectivity Parameters

Examining sex effects on intrinsic connectivity showed a negative influence from rThal to rGP in female compared to male participants across all experimental conditions (Fig. 3a). For the modulatory effects on connectivity, we found a greater self-inhibition in rThal in female than male participants in the NoGo condition (Fig. 3b). This suggests that for female participants, rThal exhibits reduced sensitivity to inputs from the other regions of the selected network during response inhibition.

Brain Behavior Associations: Inhibitory Behavioral Performance and Connectivity Parameters

Examining associations between inhibitory performance on the behavioral level (NoGo performance) and connectivity parameters revealed a very strong evidence (posterior probability > 99%) that NoGo accuracy was positively associated with the directed connectivity from rThal to rIFG.

DCM Analyses in the Left Hemisphere

To further validate the hemispheric asymmetry of the inhibitory control network, an identical model for the left hemisphere including lIFG, lCau, lGP, and lThal was tested (Fig. 4a). Participants with <10% explained variance were excluded and finally 82 participants (40 males, age: mean ± SEM = 21.24 ± 0.27 years) were included for the final DCM analyses. In contrast to the right model, no directed influences from IFG to subcortical regions were observed in terms of matrix A in the left model (Fig. 4b,f). Although the results showed modulatory effects of NoGo and Go conditions on the connectivity from IFG to Cau and Thal in both left and right models, the modulation effect of experimental condition on GP to Cau connectivity was only found in the right model (Fig. 4c,d,g,h). Additionally, the NoGo condition showed an inhibitory modulatory effect on the connectivity from Cau to GP in the left but not the right model and the Go condition showed an excitatory modulatory effect on the connectivity from Thal to IFG in the right but not the left one. Moreover, the two models had a similar pattern for the driving inputs of the NoGo condition on regions but

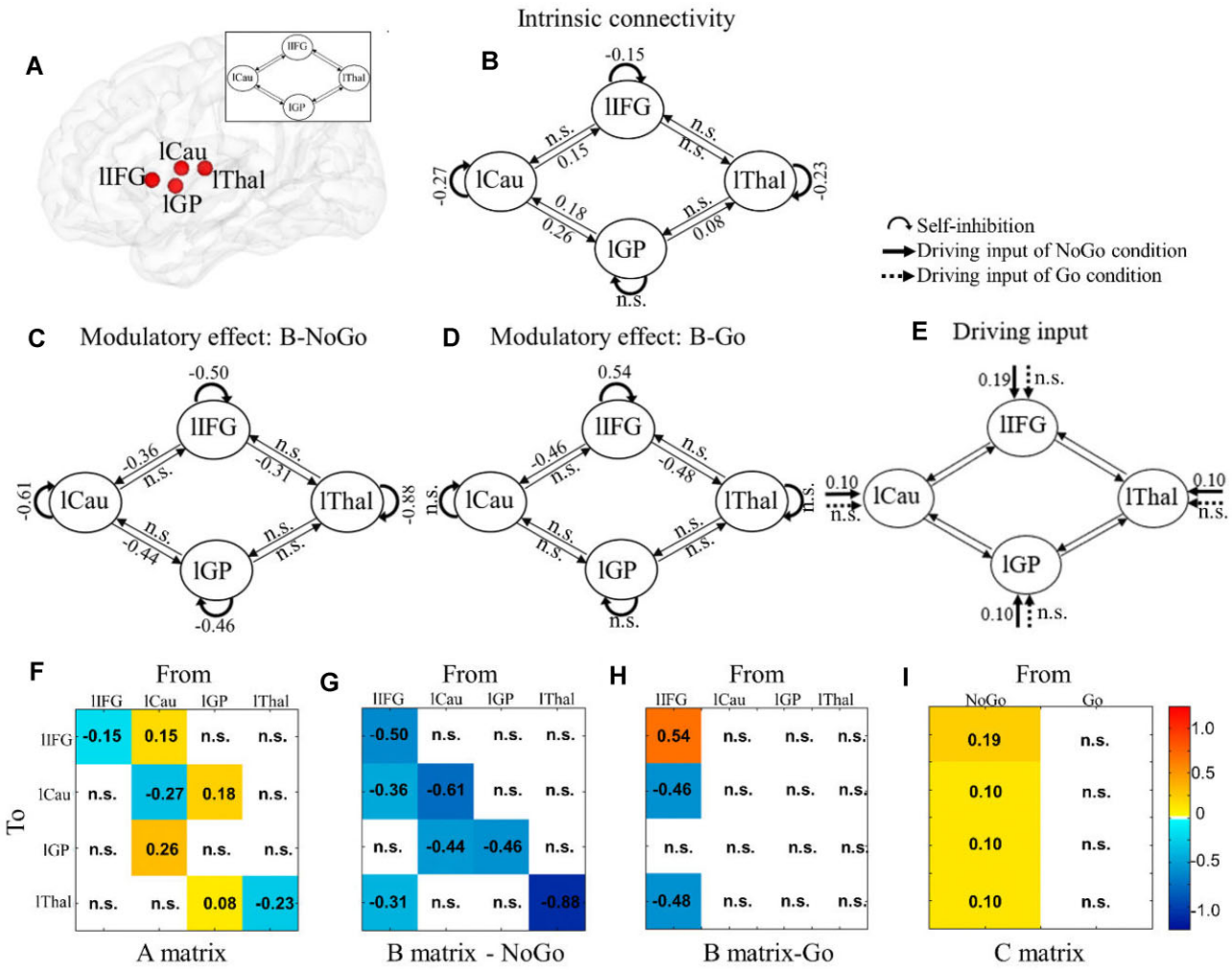

Figure 4: Location of regions included in the left model and group-level connectivity parameters. (**A**) Location of regions included in the left model. The A matrix: intrinsic connectivity independent of experimental conditions (**B**, **F**). The B matrix: modulatory effect on effective connectivity between regions and self-connections in the NoGo (**C**, **G**) and Go condition (**D**, **H**). The C matrix: driving inputs into ROI of NoGo and Go conditions (**E**, **I**). Values in matrices reflect the connectivity parameters. Effective connectivity strengths are displayed by the color ranging from yellow to dark red (i.e. excitatory connectivity) and from turquoise to dark blue (i.e. inhibitory). Parameters with stronger evidence (posterior probability > 95%) are presented and subthreshold parameters marked with "n.s.".

not the Go condition (Fig. 4e,i). The different causal structure in the left and right model indicated a hemispheric asymmetry in the inhibition network. Additional Bayesian analyses confirmed the lack of a robust cortical-subcortical pathway in the left hemisphere (Supplementary Materials).

Discussion

We capitalized on a combination of recent progress in biologically plausible causal hierarchical modeling (DCM-PEB) and a comparably large fMRI response inhibition dataset to determine causal information flow and key nodes within the extensively described basal ganglia-thalamocortical response inhibition circuits (Alexander *et al.*, 1986, 1991; Alexander and Crutcher, 1990; Aron *et al.*, 2007; Jahfari *et al.*, 2019; Morein-Zamir and Robbins, 2015; Pfeifer *et al.*, 2022; Schall and Godlove, 2012; Stuphorn, 2015; Verbruggen and Logan, 2009; Wei and Wang, 2016). Our neurocomputational model successfully validated a right-lateralized inhibitory control causal circuit and the best model showed significant intrinsic connectivity within this functional loop and captured an increasing causal influence of the cortical rIFG node on both the rCau and rThal as well as from the rGP to the rCau during inhibition. Direct comparison between different experimental conditions (e.g. NoGo and Go) revealed enhanced input into rIFG in terms of matrix C and increased connectivity from rIFG to rCau and rThal in the NoGo compared to the Go condition in terms of matrix B, suggesting a higher engagement of causal top-down cortical-to-subcortical control via the rIFG during inhibitory control. Although no sex differences were observed in inhibitory performance or BOLD activation, females exhibited decreased intrinsic connectivity from rThal to rGP and increased self-inhibition in rThal during the NoGo condition as compared to males. This indicates that a similar behavioral performance in response inhibition might be mediated by different brain processes in men and women, particularly in thalamic loops. Moreover, a higher NoGo response accuracy was associated with stronger causal information flow from the rThal to rIFG in the NoGo condition, suggesting a particular behavioral inhibitory relevance of this pathway. Finally, our findings showed different left and right model structures, suggesting a hemispheric asymmetry in the inhibitory

control network and confirming a critical role of the rIFG in implementing response inhibition. Together, these findings identified a pivotal role of the rIFG and its effective connectivity with the rCau/rThal within the basal ganglia-thalamocortical circuit during response inhibition. Given that response inhibition deficits have been observed across a wide range of mental and neurological disorders, such findings may allow a more precise determination of target regions and circuits for neuromodulation strategies and personalized intervention.

Previous studies have underscored the predictive validity of the DCM approach based on hemodynamic responses changes (Bernal-Casas *et al.*, 2017). A study by Bernal-Casas *et al.* combined optogenetic fMRI with DCM to examine cell-type-specific causal pathways among regions within the basal ganglia-thalamocortical network and found that effective connectivity pathways during D1- and D2-receptor-expressing medium spiny neuron stimulation significantly differed (Bernal-Casas *et al.*, 2017). Furthermore, the DCM approach has also been validated based on electrophysiological time series with respect to estimating activity on the synaptic or neuronal level in both animal models (Moran *et al.*, 2011; Papadopoulou *et al.*, 2017; Rosch *et al.*, 2018) and clinical studies in humans (Papadopoulou *et al.*, 2015).

In the current study, causal modeling successfully determined a right lateralized inhibitory control causal circuit encompassing the rIFG, rCau, rGP, and rThal (Aron *et al.*, 2003; Chevrier *et al.*, 2007; Hung *et al.*, 2018; Jahfari *et al.*, 2011; Thompson *et al.*, 2021). In terms of the matrix A, a significant rIFG-rCau-rGP-rThal loop was observed with rIFG exhibiting a negative influence onto rThal, alongside a positive information flow from from rThal to rGP and rCau to rIFG in the forward direction. In the backward direction, we found significant negative connectivity from rIFG to rCau and positive connectivity from rCau to rGP as well as rGP to rThal. A more lenient threshold additionally revealed rThal to rIFG connections (posterior probability of 57%). Importantly, accounting for behavioral task context revealed a significant positive modulatory effect on rIFG in both NoGo and Go condition in terms of matrix C, which was considerably stronger during response inhibition. The direct driving inputs into the rIFG are in line with its role in top-down target detection and attentional control in the context of response inhibition (Hampshire *et al.*, 2010; Krämer *et al.*, 2013) and indicate that the rIFG represents the key regulator of other nodes. Response inhibition impairments have been observed in several disorders and identification of the rIFG as critical input and top-down regulator for response inhibition opens new targets for regional or connectivity-based neuromodulation such as real-time neurofeedback, which has been established for these regions (Li *et al.*, 2019; Weiss *et al.*, 2022; Zhao *et al.*, 2019). For instance, rIFG and response inhibition deficits have been determined in ADHD (Clark *et al.*, 2007; Morein-Zamir *et al.*, 2014) and targeting the rIFG in ADHD may be a promising treatment.

In line with our hypothesis, the best model in terms of matrix B revealed strong evidence for causal effective connectivity from the rIFG to both rCau and rThal during response inhibition (posterior probability > 95%). This inhibitory pathway is consistent with previous reports on negative coupling between the rIFG and striatal regions during behavior control (Behan *et al.*, 2015; Diekhof and Gruber, 2010). Notably, direct comparison using Bayesian contrast revealed a very strong evidence (posterior probability >99%) for increased modulatory connectivity from rIFG to rCau and rThal in the NoGo condition compared to the Go condition, suggesting the rIFG's driven engagement of cortical-to-subcortical top-down control during response inhibition. Previous animal models and human neuroimaging meta-analyses have consistently identified the rIFG as a key region implicated in dopaminergic and noradrenergic modulated inhibitory regulation (Bari *et al.*, 2011; Hauber, 2010; Ott and Nieder, 2019; Pfeifer *et al.*, 2022; Terra *et al.*, 2020; Vijayraghavan *et al.*, 2016; Zhukovsky *et al.*, 2022), in particular during motor control and inhibition (Aron *et al.*, 2003; Chamberlain and Sahakian, 2007; Puiu *et al.*, 2020; Xu *et al.*, 2016). Furthermore, both fronto-striatal and fronto-thalamic projections have also been extensively involved in response inhibition (Ahissar and Oram, 2015; Bosch-Bouju *et al.*, 2013; Marzinzik *et al.*, 2008; Phillips *et al.*, 2021; Schmitt *et al.*, 2017; Sommer, 2003; Tanaka and Kunimatsu, 2011).

In addition to the cortical-subcortical pathways significant excitatory connectivity was observed from the rGP to rCau during the Go condition and switched to inhibitory connectivity when response inhibition was required during the NoGo condition. Direct comparison confirmed a considerably stronger inhibitory influence of the rGP on the rCau during response inhibition (posterior probability >99%), suggesting that communication between basal ganglia nodes is crucial for context-appropriate behavioral response control. The involvement of this pathway is in line with extensive neurophysiological evidence showing that GABA inhibitory projections from the external segment of the GP to the striatum play an essential role in cancelling a planned response when it is inappropriate (Mallet *et al.*, 2016; Wei and Wang, 2016) (but see also subthalamic nucleus to substantia nigra pars reticulata pathways in Hikosaka *et al.*, 2006; Mallet *et al.*, 2016). In addition, while numerous previous studies consistently demonstrated a right-lateralized fronto-striatal response inhibition circuit (Aron *et al.*, 2003; Chevrier *et al.*, 2007; Garavan *et al.*, 1999; Hung *et al.*, 2018; Jahfari *et al.*, 2011), the present study additionally observed an inhibitory modulation effect of the NoGo condition on the effective connectivity between the left Cau to GP, suggesting that a left lateralized basal ganglia pathway may play an important role in action restraint.

With respect to sex difference analyses, we observed that females exhibited a lower intrinsic connectivity from rThal to rGP compared to male participants in the absence of performance differences, suggesting a different baseline basal ganglia-thalamic connectivity pattern independent of experimental contexts between males and females. In addition, we also found an increased modulatory effect of the NoGo condition on self-inhibition in the rThal in female, which indicates that female participants exhibited a reduced thalamic connectivity with other regions among the inhibitory control network compared to male participants. Given that previous studies reported an important role of the thalamus in relaying information and monitoring performance via reciprocal connections with the basal ganglia and PFC (Guillery, 1995; Phillips *et al.*, 2021; Xiao *et al.*, 2009; Tanaka and Kunimatsu, 2011), our findings may reflect a higher neural efficiency of this basal ganglia-thalamocortical circuit during response inhibition in females compared to males in the context of comparable performance in both groups. Moreover, while previous findings on sex differences in response inhibition performance and the underlying neural activity remained inconsistent (Chung *et al.*, 2020; Gaillard *et al.*, 2020, 2021; Li *et al.*, 2006; Ribeiro *et al.*, 2021; Sjoberg and Cole, 2018), similar findings have been reported in a previous study using a Go/NoGo task. This study reported significant sex differences on the neural response level in terms of functional connectivity in the absence of behavioral performance differences (Chung *et al.*, 2020). However, it also has to be acknowledged that the findings by Chung *et al.*, differ in important aspects from our findings, such as those authors observed greater functional connectivity between subcortical regions including

thalamus and amygdala with other regions in females as compared to males. This may reflect the influence of age-related factors (the previous study was conducted in adolescents), given that males and females exhibit different neuromaturation of the inhibitory control circuits (Weafer, 2020). In addition, although the present findings suggest that our model was sensitive to biological variables and that separable information processes may underly response inhibition in men and women (see also Chung *et al.*, 2020; Li *et al.*, 2006), further research is needed to firmly verify the pivotal role of rIFG and its top-down control to subcortical rCau and rThal regions in response inhibition in the context of individual differences. Moreover, the functional relevance of the identified pathways was further underscored by a significant association between response inhibition performance and the causal influence from the rThal to rIFG in the NoGo condition, which demonstrates that this pathway involved in motor inhibition critically mediates behavioral success during inhibition (Wei and Wang, 2016).

Finally, our modeling tests confirmed a hemispheric asymmetry and support the critical role of right IFG circuit in response inhibition (Hung *et al.*, 2018; Jahfari *et al.*, 2011; Maizey *et al.*, 2020). The different causal structures suggest a strong cortical-subcortical intrinsic connectivity and rIFG control on the right side, although the left model revealed a different causal structure and null hypothesis tests showed moderate evidence for the difference between NoGo and Go condition's modulatory effects on effective connectivity from lIFG to lCau and to rThal (e.g. lIFG to lCau: Bayes factor = 5.47; lIFG to lThal: Bayes factor = 8.20).

There are several limitations in the current study. First, in line with our main aim we did not account for emotional valence in the DCM model, which may affect response inhibition (Schimmack and Derryberry, 2005). Second, we focused on specific nodes that were based on established basal ganglia-thalamocortical circuits proposed by Alexander (Alexander et al., 1986, 1991; Alexander and Crutcher, 1990) (see also neuroimaging meta-analysis: Hung *et al.*, 2018). Other regions such as the STN (Aron *et al.*, 2016; Aron and Poldrack, 2006; Chen *et al.*, 2020) could be integrated in future studies. Third, although DCM has advantages in testing directed connectivity and causal pathways between regions, it also has a number of limitations. For instance, the approach uses a Bayesian information procedure and as such is stringently dependent on the priors (Friston *et al.*, 2003). Moreover, the approach assumes that activity in the neurons forming an assembly is conform which does not adhere to the actual physiological properties (Friston *et al.*, 2003).

Conclusions

In conclusion, our findings demonstrated a critical role of the rIFG as well as top-down cortical-subcortical control from the rIFG to rCau and rThal in response inhibition. The nodes and pathways of the model were sensitive to biological and performance variations. The nodes and pathways may represent promising targets to improve response inhibition in mental disorders.

Author contributions

Qian Zhuang (Formal analysis, Funding acquisition, Methodology, Writing – original draft), Lei Qiao (Conceptualization, Methodology, Validation), Lei Xu (Conceptualization, Methodology, Resources), Shuxia Yao (Conceptualization, Resources), Shuaiyu Chen (Methodology, Resources), Xiaoxiao Zheng (Investigation, Validation), Jialin Li (Investigation), Meina Fu (Investigation), Keshuang Li (Investigation), Deniz Vatansever (Methodology, Validation), Stefania Ferraro (Methodology, Validation), Keith M. Kendrick (Supervision, Validation, Writing – review & editing), and Benjamin Becker (Methodology, Supervision, Validation, Writing – review & editing)

Supplementary data

Supplementary data is available at *Psychoradiology Journal* online.

Conflict of interests

K.M.K. holds the position of Editor-in-Chief and B.B. is a member of editorial board of *Psychoradiology*. They were blinded from the review process and making decisions on the manuscript. Disclaimer: Any opinions, findings, conclusions or recommendations expressed in this publication do not reflect the views of the Government of the Hong Kong Special Administrative Region or the Innovation and Technology Commission.

Acknowledgement

This work was supported by the by the National Key Research and Development Program of China (grant number: 2018YFA0701400–BB), National Natural Science Foundation of China (grant numbers 31530032–KMK, 91632117–BB, 32200904–Qian Zhuang), Key Technological Projects of Guangdong Province (grant number 2018B030335001–KMK).

References

Ahissar E, Oram T (2015) Thalamic relay or cortico-thalamic processing? Old question, new answers. *Cereb Cortex* **25**:845–8.

Alexander GE, Crutcher MD (1990) Functional architecture of basal ganglia circuits: neural substrates of parallel processing. *Trends Neurosci* **13**:266–71.

Alexander GE, Crutcher MD, DeLong MR (1991) Basal ganglia-thalamocortical circuits: parallel substrates for motor, oculomotor,"prefrontal" and "limbic" functions. *Prog Brain Res* **85**:119–46.

Alexander GE, Delong MR, Strick PL (1986) Parallel organization of functionally segregated circuits linking basal ganglia and cortex. *Annu Rev Neurosci* **9**:357–81.

Aron AR, Durston S, Eagle DM, *et al.* (2007) Converging evidence for a fronto-basal-ganglia network for inhibitory control of action and cognition. *J Neurosci* **27**:11860–4.

Aron AR, Fletcher PC, Bullmore ET, *et al.* (2003) Stop-signal inhibition disrupted by damage to right inferior frontal gyrus in humans. *Nat Neurosci* **6**:115–6.

Aron AR, Herz DM, Brown P, *et al.* (2016) Frontosubthalamic circuits for control of action and cognition. *J Neurosci* **36**:11489–95.

Aron AR, Poldrack RA (2006) Cortical and subcortical contributions to stop signal response inhibition: role of the subthalamic nucleus. *J Neurosci* **26**:2424–33.

Bari A, Mar AC, Theobald DE, *et al.* (2011) Prefrontal and monoaminergic contributions to stop-signal task performance in rats. *J Neurosci* **31**:9254–63.

Behan B, Stone A, Garavan H (2015) Right prefrontal and ventral striatum interactions underlying impulsive choice and impulsive responding. *Hum Brain Mapp* **36**:187–98.

Bencivenga F, Sulpizio V, Tullo MG, Galati G (2021) Assessing the effective connectivity of premotor areas during real vs imagined grasping: a DCM-PEB approach. *Neuroimage* **230**:117806.

Bernal-Casas D, Lee HJ, Weitz AJ, Lee JH (2017) Studying brain circuit function with dynamic causal modeling for optogenetic fMRI. *Neuron* **93**:522–532.e5.

Bosch-Bouju C, Hyland BI, Parr-Brownlie LC (2013) Motor thalamus integration of cortical, cerebellar and basal ganglia information: implications for normal and parkinsonian conditions. *Front Comput Neurosci* **7**:163.

Buschman TJ, Miller EK (2014) Goal-direction and top-down control. *Phil Trans R Soc B* **369**:20130471.

Camchong J, Dyckman KA, Chapman CE, *et al.* (2006) Basal ganglia-thalamocortical circuitry disruptions in schizophrenia during delayed response tasks. *Biol Psychiatry* **60**:235–41.

Casey BJ, Castellanos FX, Giedd JN, *et al.* (1997) Implication of right frontostriatal circuitry in response inhibition and attention-deficit/hyperactivity disorder. *J Am Acad Child Adolesc Psychiatry* **36**:374–83.

Chamberlain SR, Hampshire A, Müller U, *et al.* (2009) Atomoxetine modulates right inferior frontal activation during inhibitory control: a pharmacological functional magnetic resonance imaging study. *Biol Psychiatry* **65**:550–5.

Chamberlain SR, Sahakian BJ (2007) The neuropsychiatry of impulsivity. *Curr Opin Psychiatry* **20**:255–61.

Chang J, Hu J, Li C-SR, Yu R (2020) Neural correlates of enhanced response inhibition in the aftermath of stress. *Neuroimage* **204**:116212.

Chen W, De Hemptinne C, Miller AM, *et al.* (2020) Prefrontal-subthalamic hyperdirect pathway modulates movement inhibition in humans. *Neuron* **106**:579–588.e3. e573.

Chevrier AD, Noseworthy MD, Schachar R (2007) Dissociation of response inhibition and performance monitoring in the stop signal task using event-related fMRI. *Hum Brain Mapp* **28**: 1347–58.

Chung YS, Calhoun V, Stevens MC (2020) Adolescent sex differences in cortico-subcortical functional connectivity during response inhibition. *Cogn Affect Behav Neurosci* **20**:1–18.

Clark L, Blackwell AD, Aron AR, *et al.* (2007) Association between response inhibition and working memory in adult ADHD: a link to right frontal cortex pathology? *Biol Psychiatry* **61**:1395–401.

Collins DP, Anastasiades PG, Marlin JJ, Carter AG (2018) Reciprocal circuits linking the prefrontal cortex with dorsal and ventral thalamic nuclei. *Neuron* **98**:366–379.e4. e364.

Cross CP, Copping LT, Campbell A (2011) Sex differences in impulsivity: a meta-analysis. *Psychol Bull* **137**:97–130.

Dambacher F, Sack AT, Lobbestael J, *et al.* (2014) A network approach to response inhibition: dissociating functional connectivity of neural components involved in action restraint and action cancellation. *Eur J Neurosci* **39**:821–31.

Delong MR, Wichmann T (2015) Basal ganglia circuits as targets for neuromodulation in Parkinson disease. *JAMA Neurol* **72**:1354–60.

Diekhof EK, Gruber O (2010) When desire collides with reason: functional interactions between anteroventral prefrontal cortex and nucleus accumbens underlie the human ability to resist impulsive desires. *J Neurosci* **30**:1488–93.

Dijkstra N, Zeidman P, Ondobaka S, *et al.* (2017) Distinct top-down and bottom-up brain connectivity during visual perception and imagery. *Sci Rep* **7**:1–9.

Eagle DM, Wong JCK, Allan ME, *et al.* (2011) Contrasting roles for dopamine D1 and D2 receptor subtypes in the dorsomedial striatum but not the nucleus accumbens core during behavioral inhibition in the stop-signal task in rats. *J Neurosci* **31**:7349–56.

Fan L, Li H, Zhuo J, *et al.* (2016) The Human Brainnetome Atlas: a new brain atlas based on connectional architecture. *Cereb Cortex* **26**:3508–26.

Feng C, Becker B, Huang W, *et al.* (2018) Neural substrates of the emotion-word and emotional counting Stroop tasks in healthy and clinical populations: a meta-analysis of functional brain imaging studies. *Neuroimage* **173**:258–74.

Fernández-Espejo D, Rossit S, Owen AM (2015) A thalamocortical mechanism for the absence of overt motor behavior in covertly aware patients. *JAMA Neurol* **72**:1442–50.

Friston K, Mattout J, Trujillo-Barreto N, *et al.* (2007) Variational free energy and the Laplace approximation. *Neuroimage* **34**:220–34.

Friston KJ, Harrison L, Penny W (2003) Dynamic causal modelling. *Neuroimage* **19**:1273–302.

Friston KJ, Litvak V, Oswal A, *et al.* (2016) Bayesian model reduction and empirical Bayes for group (DCM) studies. *Neuroimage* **128**:413–31.

Gaillard A, Fehring DJ, Rossell SL (2021) A systematic review and meta-analysis of behavioural sex differences in executive control. *Eur J Neurosci* **53**:519–42.

Gaillard A, Rossell SL, Carruthers SP, *et al.* (2020) Greater activation of the response inhibition network in females compared to males during stop signal task performance. *Behav Brain Res* **386**: 112586.

Garavan H, Hester R, Murphy K, *et al.* (2006) Individual differences in the functional neuroanatomy of inhibitory control. *Brain Res* **1105**:130–42.

Garavan H, Ross TJ, Stein EA (1999) Right hemispheric dominance of inhibitory control: an event-related functional MRI study. *Proc Natl Acad Sci USA* **96**:8301–6.

Ghahremani DG, Lee B, Robertson CL, *et al.* (2012) Striatal dopamine D2/D3 receptors mediate response inhibition and related activity in frontostriatal neural circuitry in humans. *J Neurosci* **32**:7316–24.

Goldstein M, Brendel G, Tuescher O, *et al.* (2007) Neural substrates of the interaction of emotional stimulus processing and motor inhibitory control: an emotional linguistic go/no-go fMRI study. *Neuroimage* **36**:1026–40.

Guillery R (1995) Anatomical evidence concerning the role of the thalamus in corticocortical communication: a brief review. *J Anat* **187**:583.

Haber S, Mcfarland NR (2001) The place of the thalamus in frontal cortical-basal ganglia circuits. *Neuroscientist* **7**:315–24.

Haber SN, Calzavara R (2009) The cortico-basal ganglia integrative network: the role of the thalamus. *Brain Res Bull* **78**:69–74.

Hampshire A, Chamberlain SR, Monti MM, *et al.* (2010) The role of the right inferior frontal gyrus: inhibition and attentional control. *Neuroimage* **50**:1313–9.

Hampton WH, Alm KH, Venkatraman V, *et al.* (2017) Dissociable frontostriatal white matter connectivity underlies reward and motor impulsivity. *Neuroimage* **150**:336–43.

Hauber W (2010) Dopamine release in the prefrontal cortex and striatum: temporal and behavioural aspects. *Pharmacopsychiatry* **43**:S32–41.

Hikosaka O, Nakamura K, Nakahara H (2006) Basal ganglia orient eyes to reward. *J Neurophysiol* **95**:567–84.

Holmes E, Zeidman P, Friston KJ, Griffiths TD (2021) Difficulties with speech-in-noise perception related to fundamental grouping processes in auditory cortex. *Cereb Cortex* **31**:1582–96.

Huang AS, Mitchell JA, Haber SN, *et al.* (2018) The thalamus in drug addiction: from rodents to humans. *Phil Trans R Soc B* **373**:20170028.

Hung Y, Gaillard SL, Yarmak P, Arsalidou M (2018) Dissociations of cognitive inhibition, response inhibition, and emotional interference: voxelwise ALE meta-analyses of fMRI studies. *Hum Brain Mapp* **39**:4065–82.

Jahfari S, Ridderinkhof KR, Collins AGE, *et al.* (2019) Cross-task contributions of frontobasal ganglia circuitry in response inhibition and conflict-induced slowing. *Cereb Cortex* **29**:1969–83.

Jahfari S, Verbruggen F, Frank MJ, *et al.* (2012) How preparation changes the need for top–down control of the basal ganglia when inhibiting premature actions. *J Neurosci* **32**:10870–8.

Jahfari S, Waldorp L, Van Den Wildenberg WPM, *et al.* (2011) Effective connectivity reveals important roles for both the hyperdirect (fronto-subthalamic) and the indirect (fronto-striatal-pallidal) fronto-basal ganglia pathways during response inhibition. *J Neurosci* **31**:6891–9.

Kass RE, Raftery AE (1995) Bayes factors. *J Am Statist Assoc* **90**:773–95.

Kelly AMC, Hester R, Murphy K, *et al.* (2004) Prefrontal-subcortical dissociations underlying inhibitory control revealed by event-related fMRI. *Eur J Neurosci* **19**:3105–12.

Kim H (2014) Involvement of the dorsal and ventral attention networks in oddball stimulus processing: a meta-analysis. *Hum Brain Mapp* **35**:2265–84.

Klugah-Brown B, Di X, Zweerings J, *et al.* (2020) Common and separable neural alterations in substance use disorders: a coordinate-based meta-analyses of functional neuroimaging studies in humans. *Hum Brain Mapp* **41**:4459–77.

Krämer UM, Solbakk A-K, Funderud I, *et al.* (2013) The role of the lateral prefrontal cortex in inhibitory motor control. *Cortex* **49**:837–49.

Li C-SR, Huang C, Constable RT, Sinha R (2006) Gender differences in the neural correlates of response inhibition during a stop signal task. *Neuroimage* **32**:1918–29.

Li C-SR, Zhang S, Duann J-R, *et al.* (2009) Gender differences in cognitive control: an extended investigation of the stop signal task. *Brain Imag Behavior* **3**:262–76.

Li J, Xu L, Zheng X, *et al.* (2019) Common and dissociable contributions of alexithymia and autism to domain-specific interoceptive dysregulations–a dimensional neuroimaging approach. *Psychother Psychosom* **88**:187–9.

Li J, Yang X, Zhou F, *et al.* (2020) Modafinil enhances cognitive, but not emotional conflict processing via enhanced inferior frontal gyrus activation and its communication with the dorsomedial prefrontal cortex. *Neuropsychopharmacol.* **45**:1026–33.

Li K, Jiang Y, Gong Y, *et al.* (2019) Functional near-infrared spectroscopy-informed neurofeedback: regional-specific modulation of lateral orbitofrontal activation and cognitive flexibility. *Neurophoton.* **6**:1.

Liu X, Zhou X, Zeng Y, *et al.* (2022) Medial prefrontal and occipito-temporal activity at encoding determines enhanced recognition of threatening faces after 1.5 years. *Brain Struct Funct* **227**:1655–72.

Maizey L, Evans CJ, Muhlert N, *et al.* (2020) Cortical and subcortical functional specificity associated with response inhibition. *Neuroimage* **220**:117110.

Mallet N, Schmidt R, Leventhal D, *et al.* (2016) Arkypallidal cells send a stop signal to striatum. *Neuron* **89**:308–16.

Mamah D, Wang L, Barch D, *et al.* (2007) Structural analysis of the basal ganglia in schizophrenia. *Schizophr Res* **89**:59–71.

Marzinzik F, Wahl M, Schneider G-H, *et al.* (2008) The human thalamus is crucially involved in executive control operations. *J Cogn Neurosci* **20**:1903–14.

Mcfarland NR, Haber SN (2002) Thalamic relay nuclei of the basal ganglia form both reciprocal and nonreciprocal cortical connections, linking multiple frontal cortical areas. *J Neurosci* **22**:8117–32.

Moran RJ, Jung F, Kumagai T, *et al.* (2011) Dynamic causal models and physiological inference: a validation study using isoflurane anaesthesia in rodents. *PLoS ONE* **6**:e22790.

Morein-Zamir S, Robbins TW (2015) Fronto-striatal circuits in response-inhibition: relevance to addiction. *Brain Res* **1628**:117–29.

Morein-Zamir S, Dodds C, Van Hartevelt TJ, *et al.* (2014) Hypoactivation in right inferior frontal cortex is specifically associated with motor response inhibition in adult ADHD. *Hum Brain Mapp* **35**:5141–52.

Obeso JA, Rodriguez-Oroz MC, Rodriguez M, *et al.* (2000) Pathophysiology of the basal ganglia in Parkinson's disease. *Trends Neurosci* **23**:S8–S19.

Ott T, Nieder A (2019) Dopamine and cognitive control in prefrontal cortex. *Trends Cogn Sci* **23**:213–34.

Pan Y, Wang L, Zhang Y, *et al.* (2018) Deep brain stimulation of the internal globus pallidus improves response initiation and proactive inhibition in patients with Parkinson's disease. *Front Psychol* **9**:351.

Papadopoulou M, Cooray G, Rosch R, *et al.* (2017) Dynamic causal modelling of seizure activity in a rat model. *Neuroimage* **146**:518–32.

Papadopoulou M, Leite M, Van Mierlo P, *et al.* (2015) Tracking slow modulations in synaptic gain using dynamic causal modelling: validation in epilepsy. *Neuroimage* **107**:117–26.

Pfeifer P, Sebastian A, Buchholz HG, *et al.* (2022) Prefrontal and striatal dopamine D2/D3 receptors correlate with fMRI BOLD activation during stopping. *Brain Imag Behav* **16**:186–98.

Phillips JM, Kambi NA, Redinbaugh MJ, *et al.* (2021) Disentangling the influences of multiple thalamic nuclei on prefrontal cortex and cognitive control. *Neurosci Biobehav Rev* **128**:487–510.

Protopopescu X, Pan H, Altemus M, *et al.* (2005) Orbitofrontal cortex activity related to emotional processing changes across the menstrual cycle. *Proc Natl Acad Sci USA* **102**:16060–5.

Puiu AA, Wudarczyk O, Kohls G, *et al.* (2020) Meta-analytic evidence for a joint neural mechanism underlying response inhibition and state anger. *Hum Brain Mapp* **41**:3147–60.

Qiao L, Xu M, Luo X, *et al.* (2020) Flexible adjustment of the effective connectivity between the fronto-parietal and visual regions supports cognitive flexibility. *Neuroimage* **220**:117158.

Rae CL, Nombela C, Rodríguez PV, *et al.* (2016) Atomoxetine restores the response inhibition network in Parkinson's disease. *Brain* **139**:2235–48.

Raud L, Westerhausen R, Dooley N, Huster RJ (2020) Differences in unity: the go/no-go and stop signal tasks rely on different mechanisms. *Neuroimage* **210**:116582.

Renteria R, Baltz ET, Gremel CM (2018) Chronic alcohol exposure disrupts top-down control over basal ganglia action selection to produce habits. *Nat Commun* **9**:1–11.

Rey-Mermet A, Gade M, Oberauer K (2018) Should we stop thinking about inhibition? Searching for individual and age differences in inhibition ability. *J Exp Psychol Learn Mem Cogn* **44**:501.

Ribeiro F, Cavaglia R, Rato JR (2021) Sex differences in response inhibition in young children. *Cogn Dev* **58**:101047.

Robbins TW (2007) Shifting and stopping: fronto-striatal substrates, neurochemical modulation and clinical implications. *Phil Trans R Soc B* **362**:917–32.

Robertson CL, Ishibashi K, Mandelkern MA, *et al.* (2015) Striatal D1- and D2-type dopamine receptors are linked to motor response inhibition in human subjects. *J Neurosci* **35**:5990–7.

Rosch RE, Hunter PR, Baldeweg T, *et al.* (2018) Calcium imaging and dynamic causal modelling reveal brain-wide changes in effective connectivity and synaptic dynamics during epileptic seizures. *PLoS Comput Biol* **14**:e1006375.

Rubia K, Lim L, Ecker C, *et al.* (2013) Effects of age and gender on neural networks of motor response inhibition: from adolescence to mid-adulthood. *Neuroimage* **83**:690–703.
Rubia K, Smith AB, Taylor E, Brammer M (2007) Linear age-correlated functional development of right inferior fronto-striato-cerebellar networks during response inhibition and anterior cingulate during error-related processes. *Hum Brain Mapp* **28**:1163–77.
Rupprechter S, Romaniuk L, Series P, *et al.* (2020) Blunted medial prefrontal cortico-limbic reward-related effective connectivity and depression. *Brain* **143**:1946–56.
Saalmann YB, Kastner S (2015) The cognitive thalamus. *Front Syst Neurosci* **9**:39.
Schachar R, Logan GD, Robaey P, *et al.* (2007) Restraint and cancellation: multiple inhibition deficits in attention deficit hyperactivity disorder. *J Abnorm Child Psychol* **35**:229–38.
Schall JD, Godlove DC (2012) Current advances and pressing problems in studies of stopping. *Curr Opin Neurobiol* **22**:1012–21.
Schaum M, Pinzuti E, Sebastian A, *et al.* (2021) Right inferior frontal gyrus implements motor inhibitory control via beta-band oscillations in humans. *eLife* **10**:e61679.
Schimmack U (2005) Attentional interference effects of emotional pictures: threat, negativity, or arousal? *Emotion* **5**:55.
Schmitt LI, Wimmer RD, Nakajima M, *et al.* (2017) Thalamic amplification of cortical connectivity sustains attentional control. *Nature* **545**:219–23.
Sjoberg EA, Cole GG. (2018) Sex differences on the Go/No-Go test of inhibition. *Arch Sex Behav* **47**:537–42.
Sommer MA (2003) The role of the thalamus in motor control. *Curr Opin Neurobiol* **13**:663–70.
Sonuga-Barke EJS (2005) Causal models of attention-deficit/hyperactivity disorder: from common simple deficits to multiple developmental pathways. *Biol Psychiatry* **57**:1231–8.
Stephan KE, Harrison LM, Kiebel SJ, *et al.* (2007) Dynamic causal models of neural system dynamics: current state and future extensions. *J Biosci* **32**:129–44.
Stephan KE, Penny WD, Moran RJ, *et al.* (2010) Ten simple rules for dynamic causal modeling. *Neuroimage* **49**:3099–109.
Stuphorn V (2015) Neural mechanisms of response inhibition. *Curr Opin Behav Sci* **1**:64–71.
Tanaka M, Kunimatsu J (2011) Contribution of the central thalamus to the generation of volitional saccades. *Eur J Neurosci* **33**:2046–57.
Terra H, Bruinsma B, De Kloet SF, *et al.* (2020) Prefrontal cortical projection neurons targeting dorsomedial striatum control behavioral inhibition. *Curr Biol* **30**:4188–4200.e5. e4185.
Thompson A, Schel MA, Steinbeis N (2021) Changes in BOLD variability are linked to the development of variable response inhibition. *Neuroimage* **228**:117691.
Tops M, Boksem MAS (2011) A potential role of the inferior frontal gyrus and anterior insula in cognitive control, brain rhythms, and event-related potentials. *Front Psychology* **2**:330.
Van Overwalle F, Van De Steen F, Van Dun K, Heleven E (2020) Connectivity between the cerebrum and cerebellum during social and non-social sequencing using dynamic causal modelling. *Neuroimage* **206**:116326.
Verbruggen F, Logan GD (2008) Response inhibition in the stop-signal paradigm. *Trends Cogn Sci* **12**:418–24.
Verbruggen F, Logan GD (2009) Models of response inhibition in the stop-signal and stop-change paradigms. *Neurosci Biobehav Rev* **33**:647–61.
Vijayraghavan S, Major A J, Everling S (2016) Dopamine D1 and D2 receptors make dissociable contributions to dorsolateral prefrontal cortical regulation of rule-guided oculomotor behavior. *Cell Rep* **16**:805–16.
Weafer J (2020) Sex differences in neural correlates of inhibitory control. *Curr Top Behav Neurosci* **47**: 73–89.
Wei W, Wang X-J (2016) Inhibitory control in the cortico-basal ganglia-thalamocortical loop: complex regulation and interplay with memory and decision processes. *Neuron* **92**:1093–105.
Weiss F, Zhang J, Aslan A, *et al.* (2022) Feasibility of training the dorsolateral prefrontal-striatal network by real-time fMRI neurofeedback. *Sci Rep* **12**:1–10.
Xiao D, Zikopoulos B, Barbas H (2009) Laminar and modular organization of prefrontal projections to multiple thalamic nuclei. *Neuroscience* **161**:1067–81.
Xu B, Sandrini M, Wang W-T, *et al.* (2016) PreSMA stimulation changes task-free functional connectivity in the fronto-basal-ganglia that correlates with response inhibition efficiency. *Hum Brain Mapp* **37**:3236–49.
Xu L, Zheng X, Yao S, *et al.* (2022) The mirror neuron system compensates for amygdala dysfunction-associated social deficits in individuals with higher autistic traits. *Neuroimage* **251**:119010.
Zeidman P, Jafarian A, Corbin N, *et al.* (2019a) A guide to group effective connectivity analysis, part 1: first level analysis with DCM for fMRI. *Neuroimage* **200**:174–90.
Zeidman P, Jafarian A, Seghier ML, *et al.* (2019b) A guide to group effective connectivity analysis, part 2: second level analysis with PEB. *Neuroimage* **200**:12–25.
Zhang R, Geng X, Lee TMC (2017) Large-scale functional neural network correlates of response inhibition: an fMRI meta-analysis. *Brain Struct Funct* **222**:3973–90.
Zhao Z, Yao S, Li K, *et al.* (2019) Real-time functional connectivity-informed neurofeedback of amygdala-frontal pathways reduces anxiety. *Psychother Psychosom* **88**:5–15.
Zhou F, Li J, Zhao W, *et al.* (2020) Empathic pain evoked by sensory and emotional-communicative cues share common and process-specific neural representations. *eLife* **9**:e56929.
Zhou F, Zimmermann K, Xin F, *et al.* (2018) Shifted balance of dorsal versus ventral striatal communication with frontal reward and regulatory regions in cannabis-dependent males. *Hum Brain Mapp* **39**:5062–73.
Zhuang Q, Xu L, Zhou F, *et al.* (2021) Segregating domain-general from emotional context-specific inhibitory control systems-ventral striatum and orbitofrontal cortex serve as emotion-cognition integration hubs. *Neuroimage* **238**:118269.
Zhukovsky P, Morein-Zamir S, Ziauddeen H, *et al.* (2022) Prefrontal cortex activation and stopping performance underlie the beneficial effects of atomoxetine on response inhibition in healthy volunteers and those with cocaine use disorder. *Biol Psychiatr Cogn Neurosci Neuroimag* **7**:1116–26.

Received: 26 May 2023; **Revised:** 13 August 2023; **Accepted:** 12 September 2023